



Original Paper

Integration of Hydrochemistry and Stable Isotopes for Assessing Groundwater Recharge and Evaporation in Pre- and Post-Rainy Seasons in Hua County, China

Fei Xu ^{1,2,3} Peiyue Li ^{1,2,3,4} Yuanhang Wang ^{1,2,3} and Qianqian Du ^{1,2,3}

Received 15 March 2023; accepted 28 June 2023
Published online: 15 July 2023

Groundwater resource management is crucial for promoting sustainable development in areas with surface water scarcity, such as Hua County in China. This paper aims to estimate groundwater recharge and evaporation during the pre- and post-rainy seasons in Hua County. The non-equilibrium evaporation model was established to quantify the degree of evaporation. Ternary end-member mixing analysis (EMMA) was used to evaluate the contributions of recharge sources to groundwater recharge. The concentrations of major ions in surface water and groundwater showed some differences, which may be due to differences in their lithological classes and hydrogeochemical evolution. The ion concentrations of both surface water and groundwater were observed to be lower in the post-rainy season, because rainfall infiltration during the rainy season diluted ion concentrations. The Gibbs diagram, end-member diagram, and $\delta^2\text{H}$ versus $\delta^{18}\text{O}$ diagram all revealed that groundwater was affected by evaporation to some extent, especially in the pre-rainy season. The non-equilibrium evaporation model showed that the remaining proportions of evaporation calculated using ^{18}O and ^2H were 0.96 and 0.94%, respectively, during the pre-rainy season and 0.97% and 0.96%, respectively, during the post-rainy season. According to EMMA, the mean contributions of subsurface lateral flow, precipitation infiltration, and river percolation to groundwater were 47%, 28%, and 25%, respectively, during the pre-rainy season and 57%, 30%, and 13%, respectively, in the post-rainy season. The findings of the present study demonstrated that integration of hydrochemistry and isotopic signatures supports better understanding of groundwater recharge and evaporation processes.

KEY WORDS: Water–rock interaction, Non-equilibrium evaporation model, End-member mixing analysis, Deuterium excess, Hua County.

INTRODUCTION

Groundwater is the most widely used freshwater resource, particularly in areas where surface water resources are in short supply (Vadiati et al., 2018; Castano–Sanchez et al., 2020; Lall et al., 2020). Identifying groundwater recharge sources is usually difficult due to their complexity and invisibility (Gong et al., 2021). Indeed, intensive human activities and global climate change have severely affected

¹School of Water and Environment, Chang'an University, No. 126 Yanta Road, Xi'an 710054, Shaanxi, China.

²Key Laboratory of Subsurface Hydrology and Ecological Effects in Arid Region of the Ministry of Education, Chang'an University, No. 126 Yanta Road, Xi'an 710054, Shaanxi, China.

³Key Laboratory of Eco-hydrology and Water Security in Arid and Semi-arid Regions of the Ministry of Water Resources, Chang'an University, No. 126 Yanta Road, Xi'an 710054, Shaanxi, China.

⁴To whom correspondence should be addressed; e-mail: lipy2@163.com, peiyueli@chd.edu.cn

groundwater circulation and quality in several regions worldwide, resulting in several serious water resources problems, including groundwater shortage, groundwater pollution, and groundwater-related disasters (Wu et al., 2013; Chen et al., 2016; Ashraf et al., 2017; Shukla & Saxena, 2021; Snousy et al., 2022; Wei et al., 2022; Liu et al., 2022). Water resource-related problems are particularly serious in northern and northwestern China due to the dry climate conditions, low rainfall amounts, and intense human activities (Li & Qian, 2018; Li et al., 2019). Hua County is situated in the southern region of the Guanzhong Plain in northwest China, where the mean annual evaporation is greater than the rainfall, and surface water resources are in short supply, making groundwater the major source of water for domestic, industrial, and agricultural purposes (Li et al., 2016a). Clarifying the recharge and evaporation of groundwater in Hua County can provide a basis for sustainable use of local water resources and provide theoretical support for groundwater management in similar climatic regions.

Groundwater recharge can be evaluated by several approaches, including water balance, Darcian equations, water table fluctuation, tracer, and numerical modeling approaches (Wang et al., 2015, 2022). However, Darcian equations, water table fluctuation, and numerical modeling approaches require comprehensive understanding of the specific hydrogeological conditions and extensive data. Tracers can be applied to estimate groundwater recharge without extensive hydrogeological data, but their results may be uncertain. A combination of different information sources (e.g., hydrochemistry and isotope compositions) can effectively improve the reliability of groundwater recharge assessment. The hydrochemical compositions of a water body are the results of long-term interaction between it and its surrounding environments (Sefie et al., 2018; Liu et al., 2020a; Mu et al., 2023). Accordingly, assessing the hydrochemical characteristics of groundwater can determine, to some extent, the sources of major ions and their formation processes in groundwater (e.g., mineral dissolution and water filtration, mixing, and evaporation), as well as other important water cycle information. Based on factor and cluster analyses, Sun (2014) found that the hydrochemical characteristics of the Wolonghu coal mine aquifer were primarily controlled by mineral dissolution and silicate mineral weathering, while the working face water was probably recharged by water from the

loose layer and coal-bearing sandstone. Yang et al. (2022) demonstrated, using factor analysis, that hydrochemical components of groundwater in the eastern plain regions of Hotian were dominated by evaporation and concentration, as well as water-rock interactions and surface water filtration. Although hydrochemical methods can be used to identify the sources of groundwater recharge and formation processes, quantification of these processes remains challenging. Combining hydrochemical and isotopic methods is, therefore, required to provide a comprehensive explanation of groundwater recharge and evaporation processes.

Stable ^2H and ^{18}O isotopes are useful tools for identifying groundwater recharge sources (Gat, 1996; Liotta et al., 2006; Halder et al., 2015; Cheng et al., 2017; Elaid et al., 2020). Liu and Yamanaka (2012) demonstrated, using hydrochemical and isotopic methods, that rainfall, river infiltration, and mountain block recharge were the major sources of groundwater recharge in the Ashikaga area of central Japan, of which river infiltration contributed significantly to groundwater along the river by about 94%. Mohammed et al. (2014) combined isotopic and hydrochemical methods to determine the groundwater recharge relationships in the Allier River valley in France. In addition, the evaporation degree of groundwater can be determined by assessing stable ^2H and ^{18}O fractionation during the evaporation process. For example, Qian et al. (2014) showed that most lakes in the Yinchuan Plain have an evaporation proportion exceeding 25% calculated based on the non-equilibrium evaporation model. Therefore, the combination of hydrochemical and isotopic (^2H and ^{18}O) methods can help determine effectively the evaporation and recharge rates of water bodies.

Although the combination of hydrochemical and isotopic methods is a valuable approach for a systematic understanding of groundwater evaporation and recharge processes, there is a lack of studies that have used this approach in Hua County. We recognize that a single sampling event cannot fully represent the recharge and evaporation in the study area or capture their variations, and so we chose to sample separately in the pre- and post-rainy seasons. Therefore, the aims of this paper were (1) to evaluate the hydrochemical characteristics and hydrogeochemical processes of groundwater in Hua County; (2) to determine the isotopic compositions (^2H and ^{18}O) of river water and groundwater and their indications of groundwater recharge and evaporation during both seasons; and

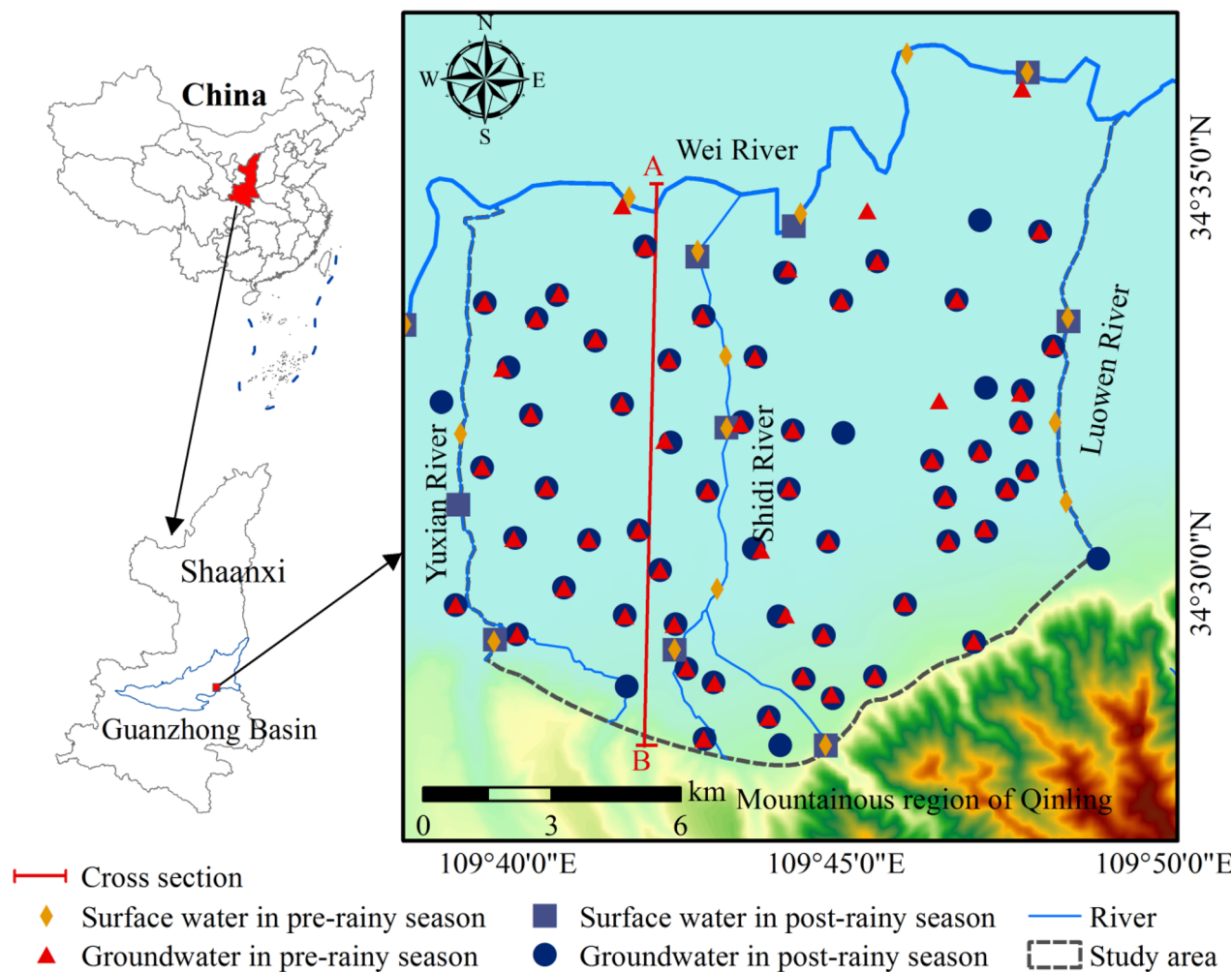


Figure 1. Location of study area and sampling points.

(3) to quantify the mean contribution of river, rainfall, and subsurface lateral flow to groundwater recharge in both seasons, as well as the extent of groundwater evaporation.

RESEARCH AREA

Study Site

Hua County is in the southern region of the Guanzhong Plain, China. The Qinling Mountains and Weihe alluvial plain are in the southern and northern regions of Hua County, respectively (Fig. 1). The landform of the area is classified into inclined pluvial and pluvial-alluvial plains in the

southern and northern parts (Du et al., 2023; Wu & Sun, 2016; Guo et al., 2023). The pluvial-alluvial plain can be divided further into three sections: the flood plain, the first terraces, and the second terraces of the Wei River. Hua County is in a region with longitude and latitude ranges of 109°39'14"–109°49'02"E and 34°27'24"–34°36'37"N, respectively, and with semi-humid continental monsoon climate (Li et al., 2016b).

Climatic and Hydrologic Characteristics

The Wei River is the largest river in the study area, with its three main tributaries flowing from the Qinling to the Wei River. A fertilizer plant exists in

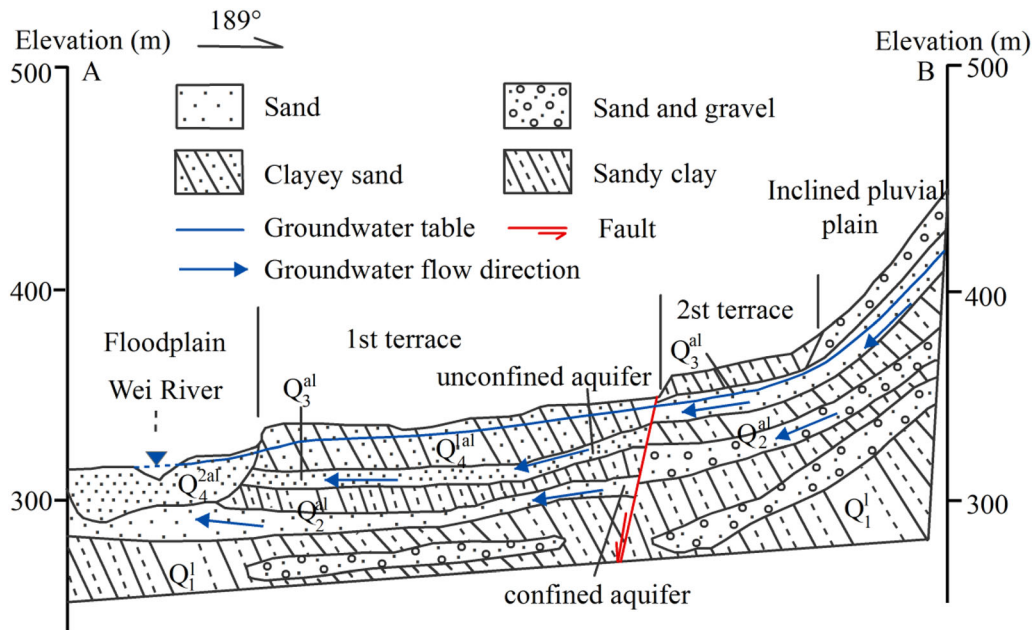


Figure 2. Hydrogeological cross section of the study area (revised after Li et al., 2016b).

Hua County; it discharges industrial wastewater, leading to the pollution of surrounding river water and groundwater (Wu & Sun, 2016). The temperature in Hua County varies from -16.5°C to 43°C , with mean annual temperature of 13.4°C (Wu & Sun, 2016), whereas rainfall and evaporation are characterized by uneven temporal distributions, with mean annual rainfall and mean evaporation of 581.2 and 830.7 mm, respectively, of which 50% and 65%, respectively, occur mainly over the July–September and April–August periods, respectively (Li et al., 2016a; Wang & Li, 2022).

Geological and Hydrogeological Characteristics

The long geological history of the region has led to the formation of thick layers of loose sediments in Hua County, providing ample capacity for groundwater storage (Li et al., 2016a). The groundwater in Hua County is primarily found in the Quaternary loose layer, which is classified into phreatic and confined aquifers. The phreatic aquifer supplies water for drinking and irrigation purposes in rural areas, while the confined aquifer supplies less water, mainly for centralized urban areas and industries (Wu & Sun, 2016). The unconfined aquifer thickness ranges from 38 to 51 m, and it consists of coarse and alluvial sands

formed in Late Pleistocene and Holocene (Q_3^{al} and Q_4^{al}) (Fig. 2), with good sorting ability and high permeability (Li et al., 2016a). Quartz, illite, plagioclase, and calcite are the main minerals of the Quaternary strata (Chen et al., 2021). The confined aquifer was deposited in the Early and Middle Pleistocene (Q_1^{c} and Q_2^{c}), with its top buried at a depth of about 50 m. The thickness of confined aquifer varies between 14 and 40 m (Xu, 2011). Due to the large burial depth of the confined aquifer, only the unconfined aquifer can be connected directly to the ground surface and receive recharge such as rainfall and river infiltration. The hydraulic connection between the phreatic aquifer and the confined aquifer is weak (Xu, 2011), and so only the phreatic aquifer is considered in this paper. The basic groundwater recharge sources in Hua County are subsurface lateral flow, rainfall infiltration, river seepage, and irrigation return flow, while groundwater is discharged by pumping, evaporation, and lateral runoff (Wang & Li, 2022).

MATERIALS AND METHODS

Data Collection and Analysis

In this investigation, 59 groundwater and 17 river water samples were collected in the pre-rainy

season (March–April) in 2018, and 63 groundwater and 10 river water samples were collected in the post-rainy season (November) in 2018. The groundwater samples were collected at a depth of 4.5–10.5 m. The coordinates of all sampling points were obtained using a portable GPS device (Fig. 1). All samples were stored in duplicate in 2.5 L polyethylene plastic bottles for hydrochemical characterization, and the water samples stored in 3 ml glass containers were filtered through 0.22 μm polyether-sulfone membrane for isotopic analyses. TDS (total dissolved solids), EC (electrical conductivity), and pH were determined *in situ* using portable meters, while the other hydrochemical indicators were tested at the Shaanxi Institute of Geological Engineering Investigation’s laboratory. The analyzed indices used in this research included K⁺, Mg²⁺, Ca²⁺, Na⁺, HCO₃⁻, SO₄²⁻, CO₃⁻, and Cl⁻. Of these, K⁺ and Na⁺ were determined with a flame photometer (GFU2202) (the detection limit was 0.02 mg/L with uncertainty of about 3%); Mg²⁺, Ca²⁺, CO₃⁻, and HCO₃⁻ were determined by titrimetric method (the detection limit was 0.01 mg/L with uncertainty of about 3%); and SO₄²⁻ and Cl⁻ were analyzed using ion chromatography (HLC2601). (The detection limit was 0.02 mg/L with uncertainty of about 3%.) The balance error (%CBE) values were within ± 5% for all water samples, indicating reliable analytical results. δD and δ¹⁸O were analyzed with a liquid water isotope analyzer (Picarro L2140-i) with analytical errors less than 0.5‰ and 0.1‰, respectively. The isotopic measurements were obtained as:

$$\delta(\%) = \frac{R_{\text{sample}} - R_{\text{standard}}}{R_{\text{standard}}} \times 1000 \quad (1)$$

Calculation of Groundwater Evaporation Losses based on Isotopic Fractionation

Water on earth is formed through multiple water cycle components, including evaporation, condensation, infiltration, and runoff (Shi et al., 2003). Indeed, isotopic fractionations occur during the different states of water because certain thermodynamic properties of the water molecule are related to the hydrogen and oxygen atom masses (Shi et al., 2003). Evaporation and condensation are two significant components of the atmospheric water cycle. During water evaporation and condensation,

the hydrogen and oxygen isotope contents change slightly and referred to as isotopic fractionation (Hu et al., 2007). Hydrogen and oxygen isotopes of water are, therefore, good tracers for studying evaporation and condensation processes. In this research, oxygen and hydrogen isotopes were used to quantify groundwater evaporation based on the Rayleigh fractionation principle, according to the following equation:

$$R_l = R_l^0 \times f^{(\alpha_{v-l}-1)} \quad (2)$$

where R_l denotes heavy-to-light isotope ratio in samples, R_l^0 denotes initial heavy-to-light isotope ratio in water samples, α_{v-l} is the fractionation coefficient from gas to liquid phases, and f denotes the remaining fraction of evaporation.

Evaporation in nature predominantly occurs as free evaporation, which is a non-equilibrium or dynamic process. Temperature is the main factor influencing isotopic fractionation under equilibrium conditions, while under non-equilibrium conditions, in addition to temperature, relative humidity and wind speed also influence isotope fractionation. Therefore, the fractionation factor was determined in this study by considering both the equilibrium and kinetic fractionation coefficients, according to the following equations:

$$\alpha_{l-v} = \varepsilon_{l-v} + \Delta\varepsilon_{bl-v} \quad (3)$$

$$\alpha_{v-l} = 1/\alpha_{l-v} \quad (4)$$

where α_{l-v} is the fractionation coefficient from liquid to gas phases, ε_{l-v} is the equilibrium fractionation coefficient, and $\Delta\varepsilon_{bl-v}$ is the kinetic fractionation coefficient.

Majoube (1971) demonstrated that the equilibrium fractionation coefficients for δ¹⁸O and δ²H depend mainly on temperature, thus:

$$\ln\varepsilon_{l-v}^{2\text{H}} = 24.844 \times 10^3 / T^2 - 76.248 / T + 52.612 \times 10^{-3} \quad (5)$$

$$\ln\varepsilon_{l-v}^{18\text{O}} = 1.137 \times 10^3 / T^2 - 0.4156 / T - 2.0667 \times 10^{-3} \quad (6)$$

where T denotes water surface temperature. The kinetic fractionation coefficient is related to the relative humidity and can be calculated as:

$$\Delta\epsilon_{bl-v}^{2H} = 12.5 \times (1 - h)/1000 \quad (7)$$

$$\Delta\epsilon_{bl-v}^{18O} = 14.2 \times (1 - h)/1000 \quad (8)$$

where h denotes atmospheric humidity. In this paper, temperature and atmospheric humidity values were obtained from the Huashan meteorological station. The mean temperature and relative humidity data in the sampling period were 17.2 °C and 45.87% in March–April and 13.5 °C and 61.13% in November, respectively.

Estimation of Contribution Ratio of End-Members

The EMMA (end-member mixing analysis) was first proposed by Hooper et al. (1990) to determine the contribution of potential water sources. This analysis has been applied extensively by several scholars (e.g., Peng et al., 2016, 2018; Li et al., 2017, Liu et al., 2020b). Wang and Li (2022) highlighted four major groundwater recharge sources in Hua County, namely subsurface lateral flow, irrigation return flow, rainfall infiltration, and river seepage. However, irrigation activity in Hua County starts mainly in the late April and continues to May each year (Li et al., 2016a), and there was no irrigation during the sampling period of this study. In addition, we considered the portion from irrigation return flow during the irrigation period as part of groundwater lateral runoff. Therefore, only three

groundwater recharge sources were considered in this study, namely rainfall, groundwater lateral inflow, and river seepage, and were used as end-members of mixing to investigate groundwater recharge characteristics in Hua County.

According to Liu and Yamanaka (2012), EMMA should follow the following assumptions: (1) steady concentration of the selected end-member substance; (2) linear mixing process; and (3) substances are conservative tracers. Indeed, chloride (Cl^-) in groundwater is a conservative tracer. Therefore, the relationship between $\delta^{18}O$ and Cl^- in all samples was drawn in this study using an EMMA diagram. If the isotopic components of the mixed groundwater (D_1) were plotted in the triangle defined by samples A, B, and C (Fig. 3a), it indicates that groundwater is recharged from three different water sources. In addition, the mixing ratio depends on the relative size of the triangles AD_1B , BD_1C , and AD_1C . The EMMA model can be expressed as:

$$(\delta^{18}O)_g = (\delta^{18}O)_s f_s + (\delta^{18}O)_p f_p + (\delta^{18}O)_l f_l \quad (9)$$

$$Cl_g^- = Cl_s^- f_s + Cl_p^- f_p + Cl_l^- f_l \quad (10)$$

$$f_s + f_p + f_l = 1 \quad (11)$$

where f_s , f_p , and f_l are proportions of infiltrated river, rainfall, and subsurface lateral runoff, respectively.

However, when samples lie outside the triangle confined by the end-members, it indicates that

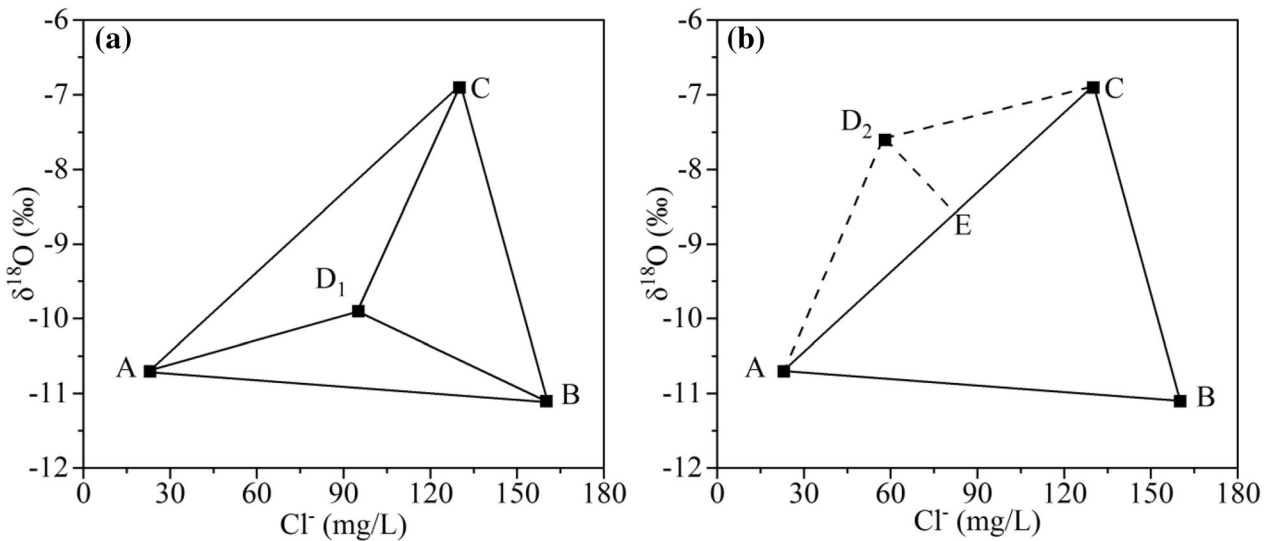


Figure 3. Schematic diagram of the end-member mixing model.

groundwater was recharged by only two sources, and the contribution of end-members to groundwater recharge is assessed using the approach proposed by Liu et al. (2004). As shown in Figure 3b, a new triangle was formed by joining the anomalous water sample D₂ with the two end-members closest to D₂. A vertical line was made through point D₂. The contribution of A and C is the CE-to-AE lengths ratio, and the model is expressed as:

$$(\delta^{18}\text{O})_g = (\delta^{18}\text{O})_{Af}f_A + (\delta^{18}\text{O})_{Cf}f_C \quad (12)$$

$$\text{Cl}_g^- = \text{Cl}_{Af}^-f_A + \text{Cl}_{Cf}^-f_C \quad (13)$$

$$f_A + f_C = 1 \quad (14)$$

where f_A and f_C are the proportions of any two end-members in infiltrated river, infiltrated rainfall, and subsurface lateral inflow.

RESULTS AND DISCUSSION

General Hydrochemical Characteristics

It is necessary to understand the major ion hydrochemical characteristics of groundwater before studying the evaporation and recharge characteristics. The values of the major physicochemical parameters of water samples from different seasons in Hua County are shown in Table 1. The mean pH of groundwater and river water in either season exceeded 7.5 and 8, respectively, which were slightly

alkaline. The possible reason for the higher mean pH of river water compared to groundwater is the existence of aquatic plants or algae in the surface water causing, which can increase pH (Wang et al., 2017). Before the rainy season, Na⁺ showed the highest concentration of 102.89 mg/L in surface water, followed by Ca²⁺, and the smallest concentration of K⁺. The ion concentrations in groundwater were ranked according to their means as Ca²⁺ > Na⁺ > Mg²⁺ > K⁺. The high concentration of Ca²⁺ in groundwater originated mainly from the dissolution of minerals such as calcite and feldspar, which are of geogenic origin and abundant within the aquifer of the study area (Li et al., 2014). Na⁺ probably originated from cation exchange and halite dissolution, owing to the prevalent occurrence of halite as a mineral in Hua County and cation exchange has been reported as hydrochemical mechanism (Li et al., 2014). In addition, Mg²⁺ is a common element in the environment. For anions, the means of HCO₃⁻, SO₄²⁻, and Cl⁻ were 364.27, 126.91, and 57.13 mg/L in groundwater and 246.75, 175.22, and 93.89 mg/L in surface water, respectively, in the pre-rainy season. The high concentration of HCO₃⁻ was derived from dissolution of carbonate minerals. The above analysis shows that the ion concentrations in river water and groundwater show some differences. Both lithological classes and geochemical evolution and the degree of hydraulic connection between river and groundwater may be responsible for the large differences in hydrochemical properties of river water and groundwater. The means of major ions were lower in

Table 1. Statistical analysis of major physicochemical indices (units: mg/L except pH dimensionless and EC μS/cm)

Parameters	Groundwater						Surface water					
	Pre-rainy season			Post-rainy season			Pre-rainy season			Post-rainy season		
	Min	Max	Mean	Min	Max	Mean	Min	Max	Mean	Min	Max	Mean
pH	7.12	8.16	7.68	6.99	8.19	7.77	7.31	8.78	8.14	7.72	8.39	8.06
TH	100	1021	399	115	981	374	125	445	313	140	415	303
TDS	240	1684	615	212	1948	577	212	968	680	204	1008	642
EC	376	2970	1023	305	3050	959	296	1623	1092	320	1803	1010
K ⁺	0.98	27.80	4.60	0.12	27.60	4.02	1.38	12.70	8.96	1.63	12.20	7.35
Na ⁺	11.40	248.00	57.45	6.42	263.00	47.02	6.20	155.00	102.89	7.12	166.00	92.62
Ca ²⁺	36.10	256.00	110.40	36.10	230	104.34	30.10	126.00	87.35	44.10	124.00	87.48
Mg ²⁺	2.43	141.00	30.02	4.86	151.00	27.39	4.86	32.80	23.12	7.29	31.60	20.54
Cl ⁻	7.09	238.00	57.13	5.67	354.00	47.95	10.60	170.00	93.89	7.09	195.00	92.24
SO ₄ ²⁻	19.20	648.00	126.91	4.80	394.00	109.86	52.80	283.00	175.22	33.60	197.00	106.18
HCO ₃ ⁻	128.00	921.00	364.27	85.40	744.00	331.67	85.40	378.00	246.75	85.40	433.00	284.44
CO ₃ ²⁻	0	0	0	0	0	0	0	42.00	6.49	0	0	0

the post-rainy season, suggesting that rainfall may recharge groundwater.

Total hardness (TH) reflects Mg^{2+} and Ca^{2+} concentrations in water (Chakraborty et al., 2021). The means of TH in groundwater and surface water were 399 and 313 mg/L, respectively, during the pre-rainy season and 374 and 303 mg/L, respectively, during the post-rainy season. Groundwater in both periods exhibited higher TH than surface water resulting from dissolution of dolomite and calcite, indicating that groundwater experienced stronger water–rock interaction. EC in groundwater ranged 376–2970 $\mu S/cm$ with mean of 1023 $\mu S/cm$ in the pre-rainy season and 305–3050 $\mu S/cm$ with mean of 909 $\mu S/cm$ in the post-rainy season (Table 1). TDS level was influenced by several factors working together (Li et al., 2011). Low TDS values were observed in the southern mountain front of Hua County, which is the upstream area of groundwater in Hua County, whereas the low TDS values may be the result of weak evaporation and insignificant water–rock interactions (Zhou et al. 2012).

Hydrogeochemical Processes

Assessing the hydrogeochemical characteristics is of great importance for explaining the origin and formation processes of groundwater. Gibbs diagram (Gibbs, 1970) has been used to analyze the evolution of surface water and recent studies have used it extensively to analyze the evolution of groundwater (Li et al., 2016c; He et al., 2019, 2021). All groundwater samples plotted within the middle region of the Gibbs diagram (Fig. 4), indicating that groundwater hydrochemistry in Hua County is dominated by rock weathering and dissolution in both seasons. In addition, samples were very close to the upper part, and one groundwater sample plotted in the evaporation dominance area. Generally, groundwater samples revealed an overall trend of upward expansion toward the evaporation dominance area, demonstrating influence of evaporation on groundwater to some extent. Solutes in groundwater initially originate from mineral dissolution due to water–rock interaction, with carbonate reaching saturation as dissolution filtration and evaporation,

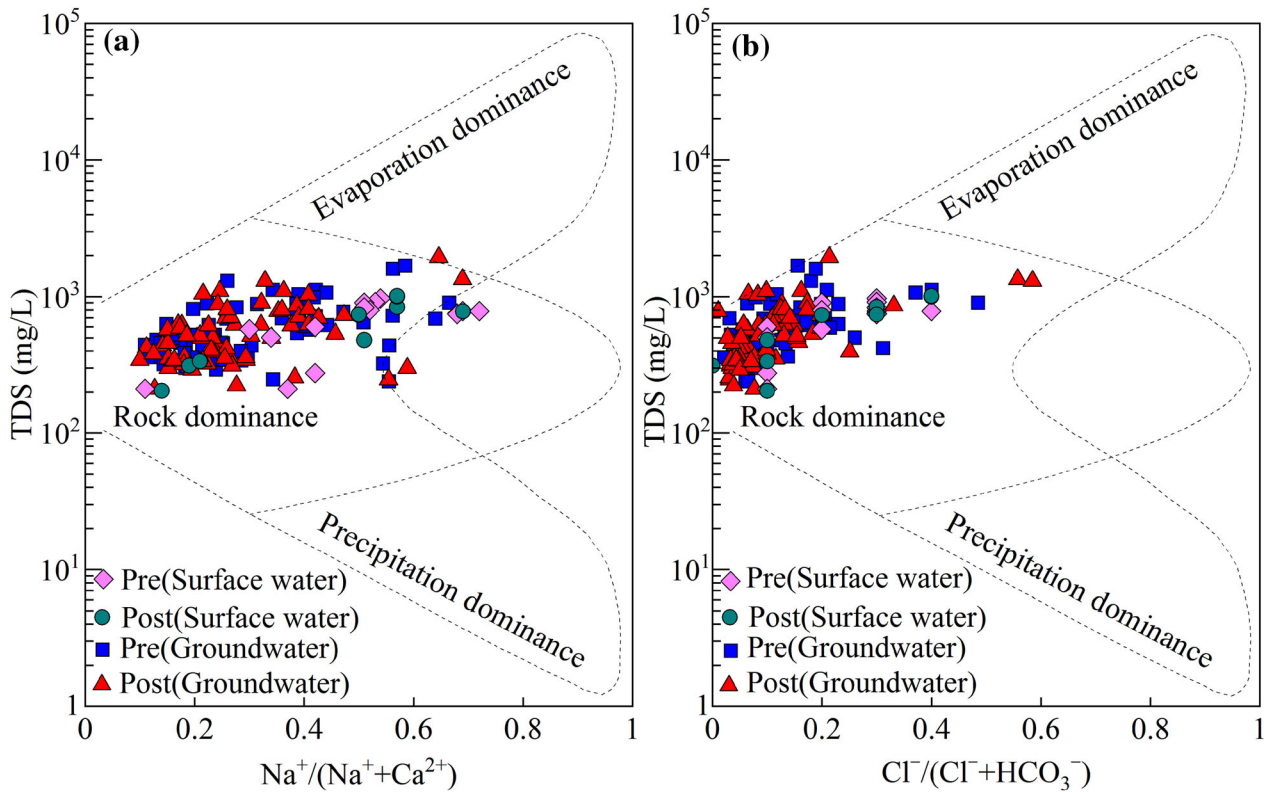


Figure 4. Gibbs diagrams of water samples.

explaining the overall trend of groundwater samples toward the evaporation dominance area of the Gibbs diagram. For the surface water samples in the study area, all of them plotted in the rock dominance zone with a trend toward the evaporation dominance zone.

Assessing ionic ratios and their interrelationships can provide further insights into the origin and formation processes of groundwater chemical components (Gong et al., 2021). End-member diagrams of Mg^{2+}/Na^+ and HCO_3^-/Na^+ with Ca^{2+}/Na^+ molar ratios can be used to identify the potential sources of chemical composition in surface water and groundwater (Gaillardet et al., 1999). As depicted in Figure 5, most groundwater samples plotted between the silicates- and carbonates-dominated areas in both seasons, indicating influences of silicates and carbonates weathering on hydrochemistry in Hua County. The groundwater samples showed a relatively wide range, indicating mixing between different rocks. The hydrochemical characteristics of groundwater were also influenced, to some extent, by evaporite dissolution, more particularly in the pre-rainy season (Fig. 5). Figure 5 also shows that surface water samples mostly plotted between the evaporites- and silicates-dominated areas and were closer to evaporites areas than groundwater samples.

Furthermore, many scholars reported that groundwater in the study area is mainly controlled by carbonate weathering dissolution and influenced by silicate weathering dissolution (Chen et al., 2021; Wang & Li., 2022).

Stable Isotopic Signatures

The isotopic compositions of rainfall are an important component of stable isotope research (Kazantseva et al., 2022; Qian et al., 2013). Indeed, Craig (1961) revealed a linear correlation between $\delta^{18}O$ and δ^2H in precipitation, known as the global meteoric water line (GMWL). The relationship between $\delta^{18}O$ and δ^2H in rainfall can be expressed as:

$$\delta^2H = 8\delta^{18}O + 10 \quad (15)$$

Qin et al. (2005) demonstrated a correlation between δ^2H and $\delta^{18}O$ in rainfall in Xi'an near the study area. This relationship can be described by the local meteoric water line (LMWL), thus:

$$\delta^2H = 7.5\delta^{18}O + 6.1 \quad (16)$$

There are some differences in the slope and intercept of LMWL compared with those of GMWL. The slope of the LMWL was slightly less

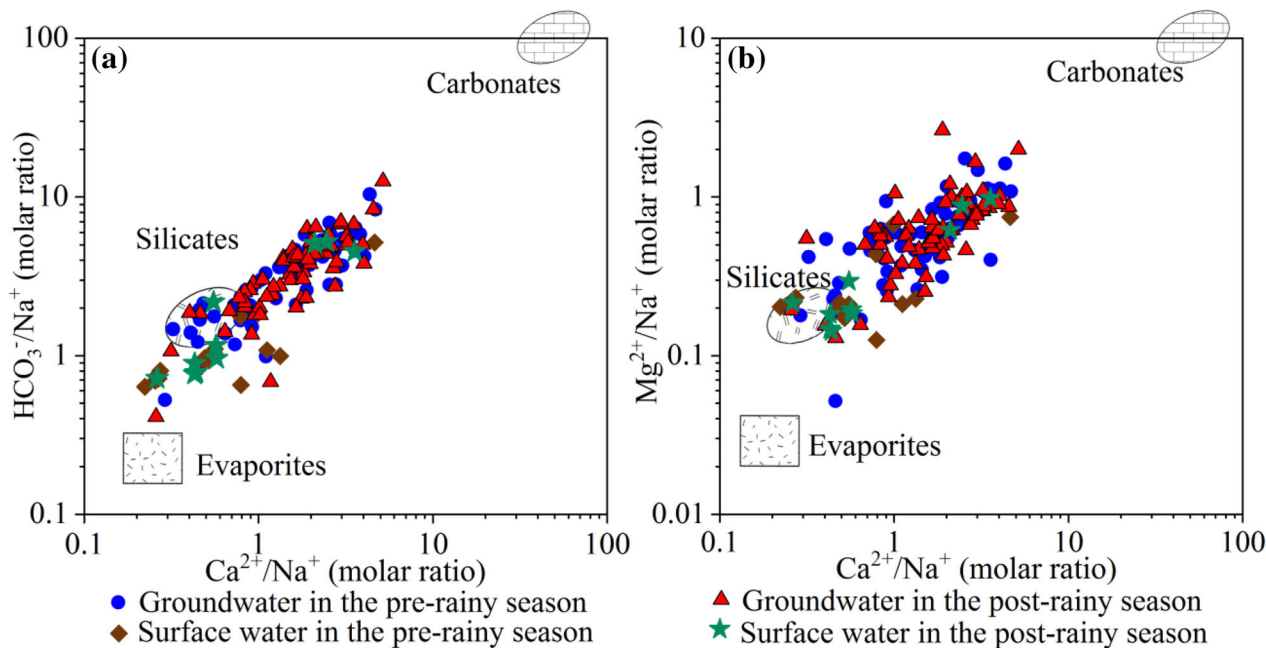


Figure 5. Relationships between different ions in water samples: (a) HCO_3^-/Na^+ vs Ca^{2+}/Na^+ ; (b) Mg^{2+}/Na^+ vs Ca^{2+}/Na^+ .

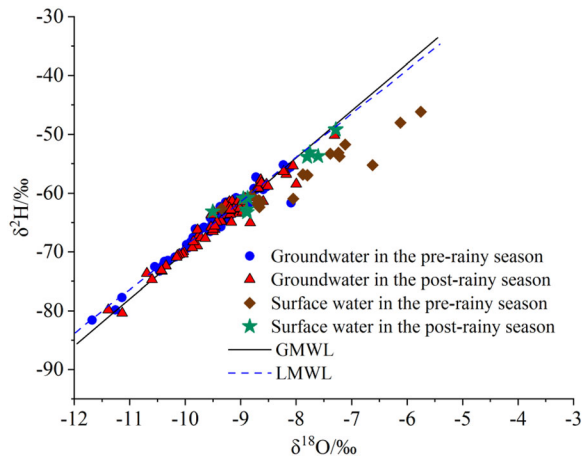


Figure 6. Plots of $\delta^2\text{H}$ versus $\delta^{18}\text{O}$ of all water bodies.

than 8, which may be due to the characteristics of Hua County. Indeed, Hua County is located in the northwest inland, where annual evaporation exceeds annual rainfall, which is more influenced by evaporation during the landing process (Jin et al., 2015). Moreover, rainfall isotopes are susceptible to non-equilibrium fractionation, resulting in heavy isotope enrichment. In this study, the observed $\delta^2\text{H}$ and $\delta^{18}\text{O}$ values in surface water and groundwater were plotted and compared with the GMWL and LMWL (Fig. 6).

Figure 6 reveals enrichment in $\delta^{18}\text{O}$ and $\delta^2\text{H}$ in river water in Hua County. In the pre-rainy season, $\delta^2\text{H}$ and $\delta^{18}\text{O}$ exhibited a range of values from -62.64‰ to -46.17‰ and from -9.34‰ to -5.75‰ , respectively, with means of -56.91‰ and -7.80‰ , respectively. In the post-rainy season, $\delta^2\text{H}$ and $\delta^{18}\text{O}$ ranged from -63.26‰ to -49.17‰ and from -9.51‰ to -7.29‰ , with means of -57.00‰ and -8.28‰ , respectively. In addition, almost all surface water samples plotted below both the LMWL and GMWL (Fig. 6), identifying evaporation trends in surface water in the study area. The samples in the pre-rainy season were distant from the LMWL, suggesting greater evaporation. The increase in $\delta^2\text{H}$ and $\delta^{18}\text{O}$ values in surface water in the pre-rainy season can potentially be attributed to low recharge rate, slow renewal, direct interaction with surface environment, and sort residence times.

Most groundwater samples in both seasons plotted along the LMWL and GMWL, suggesting that groundwater was predominantly recharged by rainfall, and there was no obvious trend toward evaporation. The means of $\delta^2\text{H}$ and $\delta^{18}\text{O}$ were

-64.77‰ and -9.42‰ , respectively, in the pre-rainy season and -64.51‰ and -9.32‰ , respectively, in the post-rainy season. The means of $\delta^{18}\text{O}$ and $\delta^2\text{H}$ in both seasons were similar, with no significant increase or decrease. Some groundwater samples showed different distributions along the LMWL, suggesting a variety of recharge sources with different isotopic signatures.

Deuterium Excess

The deuterium (D) excess is a second-order variable of $\delta^2\text{H}$ and $\delta^{18}\text{O}$, and it is significantly influenced by evaporation (Dansgaard, 1964). Strong evaporation results in a decline in the value of D-excess (Wang et al., 2020). The D-excess in groundwater reflects the degree of isotope exchange and evaporation during water-rock interactions (Yang et al., 2011; Liu et al., 2016). The D-excess can be expressed as: $d = \delta^2\text{H} - 8\delta^{18}\text{O}$. Indeed, the global mean of the D-excess is 10‰ . According to the results of this study, D-excess values in groundwater ranged from 3.11‰ to 12.68‰ and 5.59‰ to 12.88‰ , respectively, with means of 10.58‰ and 10.18‰ in the pre- and post-rainy season, respectively. The means were close to the global means, suggesting that secondary evaporation had a minor impact on groundwater in Hua County. In addition to evaporation, mixing of groundwater with other water sources (e.g., irrigation or river percolation) may also affect its isotope values (Abu Jabal et al., 2018). Moreover, the mean D-excess values in river water in the pre- and post-rainy seasons were 5.51‰ and 9.27‰ , respectively, suggesting that river water was more affected by secondary evaporation, particularly during the pre-rainy season. These findings are consistent with those revealed above.

Calculation of Evaporation Proportions

The ratio of heavy-to-light isotope in the initial groundwater sample is a crucial parameter in non-equilibrium evaporation model. Groundwater flow direction in Hua County is generally south to north and west to east. Therefore, the means of ^2H and ^{18}O isotopes of two groundwater samples in the southwestern part of Hua County were selected as initial isotopic levels.

The remaining proportions of evaporation calculated from groundwater samples in both seasons

Table 2. Calculated remaining proportions of evaporation from groundwater

Pre-rainy season						Post-rainy season					
No.	$f^{18}O$ (%)	f^2H (%)	No.	$f^{18}O$ (%)	f^2H (%)	No.	$f^{18}O$ (%)	f^2H (%)	No.	$f^{18}O$ (%)	f^2H (%)
W-01	0.97	0.94	W-37	0.96	0.95	X1-02	1.11	1.16	X1-37	0.98	0.95
W-02	0.96	0.92	W-39	0.94	0.92	X1-03	1.01	1.03	X1-38	0.93	0.90
W-03	0.96	0.91	W-44	0.96	0.91	X1-05	1.03	1.06	X1-39	0.93	0.90
W-04	0.95	0.91	W-46	0.94	0.92	X1-08	0.95	0.94	X1-40	0.98	0.98
W-05	0.90	0.84	W-47	0.90	0.85	X1-09	0.98	0.98	X2-02	0.96	0.95
W-06	0.99	0.96	W-50	0.93	0.91	X1-10	1.00	1.01	X2-03	0.99	1.00
W-07	0.95	0.91	W-52	0.94	0.90	X1-11	0.97	0.96	X2-04	1.05	1.09
W-08	1.02	1.03	W-53	0.95	0.92	X1-12	1.01	1.03	X2-05	0.97	0.93
W-09	0.99	1.00	W-54	0.93	0.91	X1-13	0.95	0.93	X2-07	0.98	0.94
W-10	0.99	0.98	W-56	0.93	0.86	X1-14	1.06	1.07	X2-08	0.92	0.93
W-11	0.95	0.92	W-57	0.99	0.97	X1-15	1.00	0.99	X2-11	0.93	0.89
W-12	1.03	1.04	W-58	0.92	0.88	X1-16	0.98	0.98	X2-12	0.94	0.92
W-13	0.94	0.90	W-60	0.99	0.99	X1-18	0.95	0.95	X2-14	0.94	0.92
W-14	0.96	0.93	W-61	0.93	0.88	X1-19	1.02	1.03	X2-15	0.95	0.94
W-15	0.96	0.93	W-62	0.93	0.88	X1-20	1.00	1.02	X2-16	0.90	0.87
W-16	0.94	0.92	W-63	0.95	0.91	X1-21	1.02	1.03	X2-17	0.92	0.89
W-19	0.94	0.90	W-67	0.95	0.90	X1-22	0.96	0.93	X2-18	0.99	1.00
W-20	0.96	0.93	W-68	0.95	0.94	X1-23	1.02	1.04	X2-19	0.95	0.95
W-21	0.92	0.88	W-69	0.96	0.96	X1-24	0.96	0.95	X2-20	0.97	0.96
W-24	0.95	0.94	W-70	1.03	1.05	X1-25	0.94	0.92	X2-21	0.92	0.90
W-25	0.97	0.95	W-71	0.94	0.91	X1-26	1.00	1.01	X2-22	0.85	0.81
W-27	0.97	0.96	W-73	0.95	0.94	X1-27	1.00	0.98	X2-23	0.95	0.92
W-28	1.02	1.04	W-74	0.99	0.99	X1-28	0.93	0.89	X2-24	0.96	0.94
W-29	0.96	0.95	W-75	0.97	0.96	X1-29	0.95	0.94	X2-25	1.04	1.07
W-32	1.10	1.16	W-76	0.97	0.97	X1-30	0.96	0.93	X2-26	0.96	0.97
W-33	1.02	1.03	W-78	0.96	0.94	X1-31	0.94	0.97	X2-27	0.95	0.93
W-34	1.00	0.99	W-79	0.97	0.96	X1-32	0.96	0.93	X2-28	0.98	0.97
W-35	1.02	1.03	W-80	0.92	0.88	X1-33	0.97	0.94	X2-29	0.98	0.98
W-36	0.96	0.96				X1-34	0.95	0.93	X2-33	0.96	0.94
						X1-35	0.90	0.88	X2-36	0.98	0.97
						X1-36	0.96	0.94			
Mean				0.96	0.94	Mean				0.97	0.96

are reported in Table 2. Although there were a few anomalies (i.e., residual evaporation ratio > 1), the overall results were reasonable. According to the results, the evaporation proportions of groundwater were low, below 6% in both seasons. The possible reasons are that the temperature during the sampling period was below 18 °C and the depth of the groundwater table was generally greater than 4 m in Hua County, which limit the evaporation process. In addition, the evaporation degrees calculated based on ¹⁸O and ²H were highly consistent, demonstrating the effectiveness of the method used in this study for quantifying evaporation in Hua County. The mean remaining proportions of evaporation based on ¹⁸O and ²H were 0.96% and 0.94%, respectively, in pre-rainy season and 0.97% and 0.96%, respectively, in post-rainy season. It is evident that there was a lower

evaporation degree in the post-rainy season, which is consistent with the above analysis.

Characteristics of Groundwater Recharge

The lateral groundwater runoff, rainfall infiltration, and river water infiltration were considered in this study as the three main end-members that contribute to groundwater recharge. The rainfall end-member was derived from the mean rainfall data collected by the Hua County Meteorological Bureau as reported by Li et al., (2016a). In addition, samples W-32 and X1-02 (upstream groundwater) were selected as end-members of subsurface lateral flow in the pre- and post-rainy season, and W38 and X2-30 represented the means of river water param-

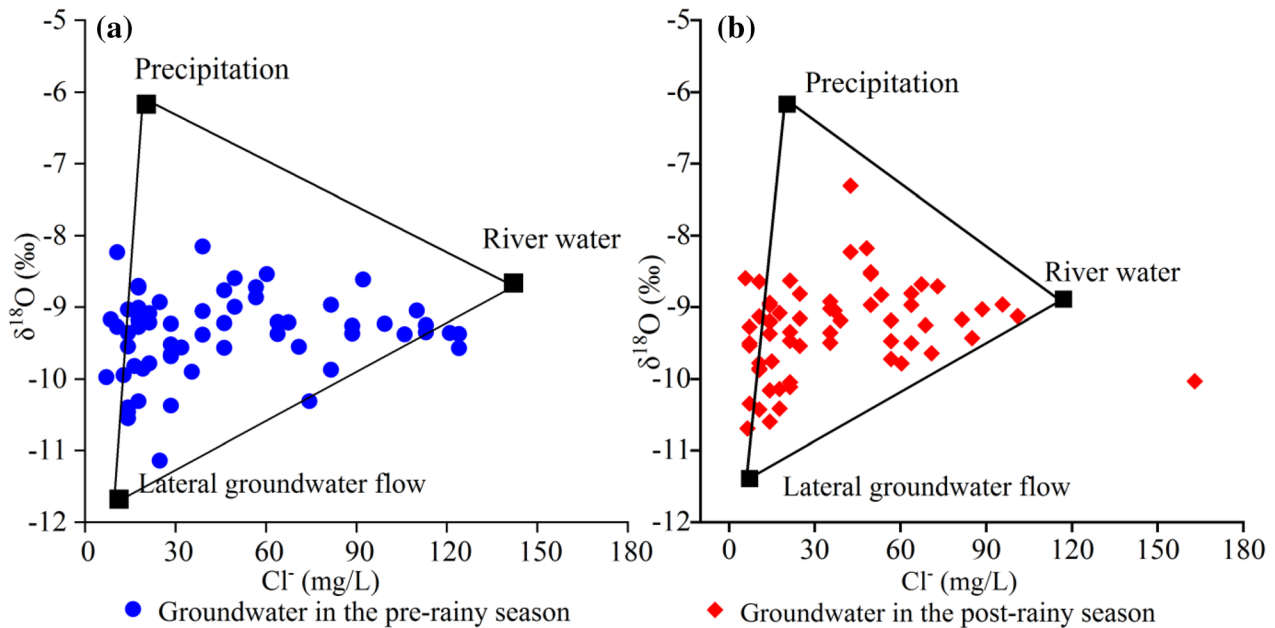


Figure 7. End-member mixing diagram of Cl^- and $\delta^{18}\text{O}$: (a) pre-rainy season; (b) post-rainy season.

eters, and so they were used as end-members of river water.

Figure 7 illustrates the correlation between Cl^- and $\delta^{18}\text{O}$ for the two seasons. Based on the results, majority of the groundwater samples lie within the triangular part consisting of the three end-members. The contributions of these end-members to groundwater recharge in Hua County were calculated using Eqs. 8–10. Groundwater samples falling outside the triangle were calculated according to Eqs. 11–13. It should be noted that one groundwater sample plotted away from the triangular area and cannot simply be assumed to be recharged by two end-members. This sample was collected near the Wei River, and a higher Cl^- value than the other samples could reasonably be interpreted as being recharged by the Wei River only or being influenced by localized effluent. According to the results, the contribution ranges of subsurface lateral flow, river water, and rainfall to groundwater recharge in the pre-rainy season were 17–86%, 0–86%, and 0–65%, respectively, with means of 47%, 25%, and 28%, respectively, whereas in the post-rainy season, corresponding end-members contributed 19–87%, 0–50%, and 4–67% to groundwater recharge, with means of 57, 13, and 30%, respectively.

It is revealed that the subsurface lateral flow was the dominant contributor to groundwater re-

charge in Hua County in both seasons, which is in line with the contribution results obtained by Li et al. (2016a) in the Shidi River of Hua County. Based on the means, the contributions of the three end-members to groundwater in both seasons followed the order of lateral groundwater flow > rainfall infiltration > surface water percolation. This finding is consistent with that obtained by Wang and Li (2022) using the water balance method, demonstrating that the selected surface water, subsurface lateral flow, and rainfall end-members in Hua County were effective in the calculation of contribution to groundwater recharge. In addition, the outcome of this paper revealed a slight increase in the contribution of precipitation to groundwater recharge in the post-rainy season, which is consistent with actual conditions.

LIMITATIONS OF THE STUDY

It should be noted that there are uncertainties when estimating the recharge contribution via the EMMA. The first is the selection of end-member samples, which is still subjective in spite of adequate consultancy to experts and relevant literature. The second is the consideration of recharge sources. Here, we chose only three main sources of recharge,

but there still are some minor sources requiring attention such as condensation of water vapor in the atmosphere and soil because there is significant temperature difference in the night and during daytime. In addition, there are uncertainties in the model itself. The model assumes there are no hydrochemical reactions before the mixing of different sources, thus overestimating the mixing proportion. However, the use of this model provides a referenceable relative value, and the findings are highly consistent with previous reports, which we believe are reasonable. In future studies, we plan to collect more high-precision hydrogeological data to set up numerical models to further quantify the absolute recharge amount of each recharge source.

CONCLUSIONS

The purposes of this paper were to evaluate the hydrochemical and isotopic features of river water and groundwater in Hua County and to quantify groundwater recharge and evaporation in different seasons based on hydrochemical and isotopic methods. The following main conclusions were obtained.

(1) Under the influence of rainfall, ion concentrations in surface water and groundwater decrease in the post-rainy season. The hydrochemical characteristics of surface water and groundwater show some differences, which may be due to different lithological classes and hydrogeochemical evolution. Groundwater hydrochemistry in Hua County is primarily dominated by rock weathering and mineral dissolution, and it is impacted, to some extent, by evaporation.

(2) The river water samples exhibit deviation from the GMWL and LMWL and are obviously affected by evaporation, while groundwater samples are distributed along the GMWL and LMWL. In addition, D-excess values of groundwater in both seasons were similar to the global mean, indicating low impact of secondary evaporation on groundwater in Hua County.

(3) Influenced by climate, groundwater evaporation in the pre-rainy season was higher than in the post-rainy season, but overall evaporation is not significant. The remaining evaporation ratios calculated using the non-equilibrium evaporation model based on ^2H and ^{18}O were 0.94% and 0.96%, respectively, in the pre-rainy season and 0.96% and 0.97%, respectively, in the post-rainy season.

(4) The EMMA using isotope and chloride tracers reveals that subsurface lateral flow had the highest contribution to groundwater recharge, with 47% and 57% in the pre- and post-rainy season, respectively. The contributions of rainfall and river water to groundwater were similar in the pre-rainy season, at 28% and 25%, respectively. After rainfall, the contribution of rainfall increased to 30%, while the contribution of surface water was only 13%.

ACKNOWLEDGMENTS

The authors are grateful for the financial support granted by the National Natural Science Foundation of China [42072286 and 41761144059]; the Qinchuangyuan “Scientist + Engineer” Team Development Program of the Shaanxi Provincial Department of Science and Technology [2022KXJ-005]; the Fok Ying Tong Education Foundation [161098]; the Fundamental Research Funds for the Central Universities of CHD [300102299301], and the National Ten Thousand Talent Program [W03070125].

DECLARATIONS

Conflict of Interest The authors declare that they have no conflict of interest.

REFERENCES

- Abu Jabal, M. S., Abustan, I., Rozaimy, M. R., & El Najar, H. (2018). The deuterium and oxygen-18 isotopic composition of the groundwater in Khan Younis City, southern Gaza Strip (Palestine). *Environmental Earth Sciences*, 77(4), 155.
- Ashraf, B., AghaKouchak, A., Alizadeh, A., Baygi, M. M., Mof-takhari, H. R., Mirchi, A., Anjileli, H., & Madani, K. (2017). Quantifying anthropogenic stress on groundwater resources. *Scientific Reports*, 7, 12910.
- Castano-Sanchez, A., Hose, G. C., & Reboleira, A. S. P. S. (2020). Salinity and temperature increase impact groundwater crustaceans. *Scientific Reports*, 10(1), 12328.
- Chakraborty, B., Roy, S., Bera, A., Adhikary, P. P., Bera, B., Sengupta, D., Bhunia, G. S., & Shit, P. K. (2021). Eco-restoration of river water quality during COVID-19 lockdown in the industrial belt of eastern India. *Environmental Science and Pollution Research*, 28(20), 25514–25528.
- Chen, J., Gao, Y., Qian, H., Ren, W., & Qu, W. (2021). Hydro-geochemical evidence for fluoride behavior in groundwater and the associated risk to human health for a large irrigation plain in the Yellow River Basin. *Science of the Total Environment*, 800, 149428.

- Chen, M., Qin, X., & Zeng, G. (2016). Impacts of human activity modes and climate on heavy metal "spread" in groundwater are biased. *Chemosphere*, *152*, 439–445.
- Cheng, Z. S., Zhang, Y. B., Su, C., & Chen, Z. (2017). Chemical and isotopic response to intensive groundwater abstraction and its implications on aquifer sustainability in Shijiazhuang, China. *Journal of Earth Science*, *28*(3), 523–534.
- Craig, H. I. (1961). Isotopic variations in meteoric waters. *Science*, *133*(3465), 1702–1703.
- Dansgaard, W. (1964). Stable isotopes in precipitation. *Tellus*, *16*, 436–468.
- Du, Q., Wu, J., Xu, F., Yang, Y., & Li, F. (2023). Occurrence, species, and health effects of groundwater arsenic in typical rural areas along the northern foot of the Qinling Mountains, China. *Exposure and Health*. <https://doi.org/10.1007/s12403-023-00576-7>.
- Elaid, M., Hind, M., Abdelmadiid, B., & Mohamed, M. (2020). Contribution of hydrogeochemical and isotopic tools to the management of upper and middle Chelif aquifers. *Journal of Earth Science*, *31*(5), 993–1006. <https://doi.org/10.1007/s12583-020-1293-y>.
- Gaillardet, J., Dupre, B., Louvat, P., & Allegre, C. J. (1999). Global silicate weathering and CO₂ consumption rates deduced from the chemistry of large rivers. *Chemical Geology*, *159*(1–4), 3–30.
- Gat, J. R. (1996). Oxygen and hydrogen Isotopes in the hydrologic cycle. *Annual Review of Earth and Planetary Sciences*, *24*, 225–262.
- Gibbs, R. J. (1970). Mechanisms controlling world water chemistry. *Science*, *17*, 1088–1090.
- Gong, Y., Liu, X., Ma, B., Qi, P., & Li, Y. (2021). Using geochemistry and environmental tracers to study shallow unconfined aquifer recharge and mineralization processes in the Yinchuan Plain, arid Northwest China. *Hydrology Research*, *52*(3), 658–675.
- Guo, W., Li, P., Du, Q., Zhou, Y., Xu, D., & Zhang, Z. (2023). Hydrogeochemical processes regulating the groundwater geochemistry and human health risk of groundwater in the rural areas of the Wei River Basin, China. *Exposure and Health*. <https://doi.org/10.1007/s12403-023-00555-y>.
- Halder, J., Terzer, S., Wassenaar, L. I., Araguas-Araguas, L. J., & Aggarwal, P. K. (2015). The Global Network of Isotopes in Rivers (GNIR): Integration of water isotopes in watershed observation and riverine research. *Hydrology and Earth System Sciences*, *19*(8), 3419–3431.
- He, X., Wu, J., & He, S. (2019). Hydrochemical characteristics and quality evaluation of groundwater in terms of health risks in Luohe aquifer in Wuqi County of the Chinese Loess Plateau, northwest China. *Human and Ecological Risk Assessment*, *25*(1–2), 32–51. <https://doi.org/10.1080/10807039.2018.1531693>.
- He, X., Li, P., Wu, J., Wei, M., Ren, X., & Wang, D. (2021). Poor groundwater quality and high potential health risks in the Datong Basin, northern China: Research from published data. *Environmental Geochemistry and Health*, *43*(2), 791–812. <https://doi.org/10.1007/s10653-020-00520-7>.
- Hooper, R. P., Christophersen, N., & Peters, N. E. (1990). Modelling streamwater chemistry as a mixture of soilwater end-members—An application to the Panola Mountain catchment, Georgia, USA. *Journal of Hydrology*, *116*(1–4), 321–343.
- Hu, H., Bao, W., Qu, S., & Wang, T. (2007). Fractionation mechanism of stable hydrogen and oxygen isotope in water body evaporating. *Journal of China Hydrology*, *27*(3), 1–5. (in Chinese).
- Jin, X., Zhang, M., Wang, S., Zhu, X., Dong, L., Ren, Z., & Chen, F. (2015). Effect of below-cloud secondary evaporation in precipitations over the Loess Plateau based on the stable isotopes of hydrogen and oxygen. *Environmental Science*, *36*(4), 8. (in Chinese).
- Kong, F., Song, J., Zhang, Y., Fu, G., Cheng, D., Zhang, G., & Xue, Y. (2019). Surface water-groundwater interaction in the Guanzhong section of the Weihe River Basin, China. *Groundwater*, *57*(4), 647–660.
- Kazantseva, A. S., Kadebskaya, O. I., & Dublyansky, Y. V. (2022). Isotopic composition of atmospheric precipitation in the Cis-Ural region. *Journal of Earth Science*, *33*, 831–838. <https://doi.org/10.1007/s12583-021-1429-8>.
- Lall, U., Josset, L., & Russo, T. (2020). A snapshot of the world's groundwater challenges. *Annual Review of Environment and Resources*, *45*, 171–194.
- Li, P., & Qian, H. (2018). Water resources research to support a sustainable China. *International Journal of Water Resources Development*, *34*(3), 327–336. <https://doi.org/10.1080/07900627.2018.1452723>.
- Li, P., Qian, H., & Wu, J. (2011). Hydrochemical characteristics and evolution laws of drinking groundwater in Pengyang County, Ningxia, Northwest China. *E-Journal of Chemistry*, *8*(2), 565–575.
- Li, P., Qian, H., Wu, J., Chen, J., Zhang, Y., & Zhang, H. (2014). Occurrence and hydrogeochemistry of fluoride in alluvial aquifer of Weihe River. *China Environmental Earth Sciences*, *71*(7), 3133–3145.
- Li, P., Wu, J., & Qian, H. (2016a). Preliminary assessment of hydraulic connectivity between river water and shallow groundwater and estimation of their transfer rate during dry season in the Shidi River, China. *Environmental Earth Sciences*, *75*(2), 99. <https://doi.org/10.1007/s12665-015-4949-7>.
- Li, P., Wu, J., & Qian, H. (2016b). Hydrochemical appraisal of groundwater quality for drinking and irrigation purposes and the major influencing factors: a case study in and around Hua County, China. *Arabian Journal of Geosciences*, *9*(1), 15. <https://doi.org/10.1007/s12517-015-2059-1>.
- Li, P., Wu, J., Qian, H., Zhang, Y., Yang, N., Jing, L., & Yu, P. (2016c). Hydrogeochemical characterization of groundwater in and around a wastewater irrigated forest in the south-eastern edge of the Tengger desert, Northwest China. *Exposure and Health*, *8*(3), 331–348. <https://doi.org/10.1007/s12403-016-0193-y>.
- Li, P., He, X., & Guo, W. (2019). Spatial groundwater quality and potential health risks due to nitrate ingestion through drinking water: A case study in Yan'an City on the Loess Plateau of northwest China. *Human and Ecological Risk Assessment*, *25*(1–2), 11–31.
- Li, X., Ye, S., Wang, L., & Zhang, J. (2017). Tracing groundwater recharge sources beneath a reservoir on a mountain-front plain using hydrochemistry and stable isotopes. *Water Science and Technology-Water Supply*, *17*(5), 1447–1457.
- Liotta, M., Favara, R., & Valenza, M. (2006). Isotopic composition of the precipitations in the central Mediterranean: Origin marks and orographic precipitation effects. *Journal of Geophysical Research-Part D-Atmospheres*, *111*(19), 1–12.
- Liu, F., Williams, M. W., & Caine, N. (2004). Source waters and flow paths in an alpine catchment, Colorado Front Range, United States. *Water Resources Research*, *40*(9), W09401.
- Liu, G., Ma, F., Liu, G., Guo, J., Duan, X., & Gu, H. (2020a). Quantification of water sources in a coastal gold mine through an end-member mixing analysis combining multivariate statistical methods. *Water*, *12*(2), 580.
- Liu, K., Qian, X., Li, B., Sun, Y., Li, Z., & Pu, C. (2016). Characteristics of deuterium excess parameters for geothermal water in Beijing. *Environmental Earth Sciences*, *75*(23), 1485.
- Liu, L., Wu, J., He, S., & Wang, L. (2022). Occurrence and distribution of groundwater fluoride and manganese in the Weining Plain (China) and their probabilistic health risk quantification. *Exposure and Health*, *14*(2), 263–279.
- Liu, M., He, T., Wu, Q., & Guo, Q. (2020b). Hydrogeochemistry of geothermal waters from Xiongan New Area and its indi-

- ating significance. *Earth Science*, 45(6), 2221–2231. (in Chinese).
- Liu, Y., & Yamanaka, T. (2012). Tracing groundwater recharge sources in a mountain–plain transitional area using stable isotopes and hydrochemistry. *Journal of Hydrology*, 464, 116–126.
- Majoube, M. (1971). Fractionnement en oxygène 18 et en deutérium entre l'eau et sa vapeur. *Journal of Chemical Physics*, 68(1971), 1423–1436.
- Mohammed, N., Celle-Jeanton, H., Huneau, F., Le Coustumer, P., Lavastre, V., Bertrand, G., Charrier, G., & Clauzet, M. L. (2014). Isotopic and geochemical identification of main groundwater supply sources to an alluvial aquifer, the Allier River valley (France). *Journal of Hydrology*, 508, 181–196.
- Mu, D., Wu, J., Li, X., Xu, F., & Yang, Y. (2023). Identification of the spatiotemporal variability and pollution sources for potential pollutants of the Malian River water in northwest China using the PCA-APCS-MLR receptor model. *Exposure and Health*. <https://doi.org/10.1007/s12403-023-00537-0>.
- Peng, T. R., Huang, C. C., Chen, J. E., Zhan, W. J., Chiang, W., & Chang, L. C. (2016). Evaluating the relative importance of groundwater recharge sources in a subtropical alluvial plain using tracer-based ternary end member mixing analysis (EMMA). *Water Resources Management*, 30(11), 3861–3878.
- Peng, T. R., Zhan, W. J., Tong, L. T., Chen, C. T., Liu, T. S., & Lu, W. C. (2018). Assessing the recharge process and importance of montane water to adjacent tectonic valley–plain groundwater using a ternary end-member mixing analysis based on isotopic and chemical tracers. *Hydrogeology Journal*, 26(6), 2041–2055.
- Qian, H., Li, P., Wu, J., & Zhou, Y. (2013). Isotopic characteristics of precipitation, surface and ground waters in the Yinchuan plain, Northwest China. *Environmental Earth Sciences*, 70(1), 57–70.
- Qian, H., Wu, J., Zhou, Y., & Li, P. (2014). Stable oxygen and hydrogen isotopes as indicators of lake water recharge and evaporation in the lakes of the Yinchuan Plain. *Hydrological Processes*, 28(10), 3554–3562.
- Qin, D. J., Turner, J. V., & Pang, Z. H. (2005). Hydrogeochemistry and groundwater circulation in the Xi'an geothermal field, China. *Geothermics*, 34(4), 471–494.
- Sefie, A., Aris, A. Z., Ramli, M. F., Narany, T. S., Shamsuddin, M. K. N., Saadudin, S. B., & Zali, M. A. (2018). Hydrogeochemistry and groundwater quality assessment of the multi-layered aquifer in Lower Kelantan Basin, Kelantan, Malaysia. *Environmental Earth Sciences*, 77(10), 397.
- Shi, H., Liu, S., & Zhao, X. (2003). Application of stable hydrogen and oxygen isotope in water circulation. *Journal of Soil and Water Conservation*, 17(2), 163–166. (in Chinese).
- Shukla, S., & Saxena, A. (2021). Appraisal of groundwater quality with human health risk assessment in parts of indo-gangetic alluvial plain, north India. *Archives Environmental Contamination and Toxicology*, 80(1), 55–73.
- Snousy, M. G., Wu, J., Su, F., Abdelhalim, A., & Ismail, E. (2022). Groundwater quality and its regulating geochemical processes in Assiut Province, Egypt. *Exposure and Health*, 14(2), 305–323. <https://doi.org/10.1007/s12403-021-00445-1>.
- Sun, L. H. (2014). Statistical analysis of hydrochemistry of groundwater and its implications for water source identification: A case study. *Arabian Journal of Geosciences*, 7(9), 3417–3425.
- Vadiati, M., Adamowski, J., & Beynaghi, A. (2018). A brief overview of trends in groundwater research: Progress towards sustainability? *Journal of Environmental Management*, 223, 849–851.
- Wang, B. G., Jin, M. G., & Liang, X. (2015). Using EARTH model to estimate groundwater recharge at five representative zones in the Hebei plain, China. *Journal of Earth Science*, 26(3), 425–434.
- Wang, P., Hu, G., & Cao, J. H. (2017). Stable carbon isotopic composition of submerged plants living in karst water and its eco-environmental importance. *Aquatic Botany*, 140, 78–83.
- Wang, S., He, X., Ding, Y., Chang, F., Wu, J., Hu, Z., Wang, L., Yang, G., & Deng, M. (2020). Characteristics and influencing factors of stable hydrogen and oxygen isotopes in groundwater in the permafrost region of the source region of the Yangtze River. *Environmental Science*, 41(1), 7. (in Chinese).
- Wang, Y., & Li, P. (2022). Appraisal of shallow groundwater quality with human health risk assessment in different seasons in rural areas of the Guanzhong Plain (China). *Environmental Research*, 207, 112210.
- Wang, J., Jin, M., Jia, B., & Kang, F. (2022). Numerical investigation of residence time distribution for the characterization of groundwater flow system in three dimensions. *Journal of Earth Science*, 33, 1583–1600. <https://doi.org/10.1007/s12583-022-1623-3>.
- Wei, M., Wu, J., Li, W., Zhang, Q., Su, F., & Wang, Y. (2022). Groundwater geochemistry and its impacts on groundwater arsenic enrichment, variation, and health risks in Yongning County, Yinchuan Plain of northwest China. *Exposure and Health*, 14(2), 219–238. <https://doi.org/10.1007/s12403-021-00391-y>.
- Wu, J., Li, P., & Qian, H. (2013). Variations of hydrogeochemical characteristics of shallow groundwater caused by agricultural activities. *Asian Journal of Chemistry*, 25(13), 7441–7444.
- Wu, J., & Sun, Z. (2016). Evaluation of shallow groundwater contamination and associated human health risk in an alluvial plain impacted by agricultural and industrial activities, mid-west China. *Exposure and Health*, 8(3), 311–329. <https://doi.org/10.1007/s12403-015-0170-x>.
- Xu, J. (2011). Study on Rational Exploitation and Utilization of Groundwater Resources of Weisan Village Drinking Water Area in Hua County. A dissertation submitted for the degree of master, Chang'an University, Xi'an. (in Chinese).
- Yang, Q., Xiao, H., Zhao, L., Yang, Y., Li, C., Zhao, L., & Yin, L. (2011). Hydrological and isotopic characterization of river water, groundwater, and groundwater recharge in the Heihe River Basin, northwestern China. *Hydrological Processes*, 25(8), 1271–1283.
- Yang, R., Zhou, J., Wei, X., Chen, Y., Lei, M., & Chen, J. (2022). Hydrochemical characteristics and evolution of groundwater in the eastern plain of Hotian Prefecture, Xinjiang. *Environmental Chemistry*, 41(4), 1367–1379. (in Chinese).
- Zhou, Z., Zhang, G., Yan, M., & Wang, J. (2012). Spatial variability of the shallow groundwater level and its chemistry characteristics in the low plain around the Bohai Sea, North China. *Environmental Monitoring Assessment*, 184(6), 3697–3710.

Springer Nature or its licensor (e.g. a society or other partner) holds exclusive rights to this article under a publishing agreement with the author(s) or other rightsholder(s); author self-archiving of the accepted manuscript version of this article is solely governed by the terms of such publishing agreement and applicable law.